AIP | Applied Physics Letters

Evaluation of photovoltaic materials within the Cu-Sn-S family

Pawel Zawadzki, Lauryn L. Baranowski, Haowei Peng, Eric S. Toberer, David S. Ginley, W. Tumas, Andriy Zakutayev, and Stephan Lany

Citation: Applied Physics Letters **103**, 253902 (2013); doi: 10.1063/1.4851896
View online: http://dx.doi.org/10.1063/1.4851896
View Table of Contents: http://scitation.aip.org/content/aip/journal/apl/103/25?ver=pdfcov
Published by the AIP Publishing

Evaluation of photovoltaic materials within the Cu-Sn-S family

Pawel Zawadzki,[1] Lauryn L. Baranowski,[1,2] Haowei Peng,[1] Eric S. Toberer,[1,2] David S. Ginley,[1] W. Tumas,[1] Andriy Zakutayev,[1,a)] and Stephan Lany[1,b)]
[1]*National Renewable Energy Laboratory, Golden, Colorado 80401, USA*
[2]*Physics Department, Colorado School of Mines, Golden, Colorado 80401, USA*

(Received 15 October 2013; accepted 27 November 2013; published online 18 December 2013)

Next-generation thin film solar cell technologies require earth abundant photovoltaic absorber materials. Here we demonstrate an alternative approach to design of such materials, evaluating candidates grouped by constituent elements rather than underlying crystal structures. As an example, we evaluate thermodynamic stability, electrical transport, electronic structure, optical and defect properties of Cu-Sn-S candidates using complementary theory and experiment. We conclude that Cu_2SnS_3 avoids many issues associated with the properties of Cu_4SnS_4, $Cu_4Sn_7S_{16}$, and other Cu-Sn-S materials. This example demonstrates how this element-specific approach quickly identifies potential problems with less promising candidates and helps focusing on the more promising solar cell absorbers. © *2013 AIP Publishing LLC*. [http://dx.doi.org/10.1063/1.4851896]

Current thin-film solar absorbers such as $Cu(In/Ga)Se_2$ (CIGS) or CdTe, although remarkably efficient[1] as polycrystalline materials incorporate limited-supply elements like indium or tellurium.[2,3] Meeting the scalability criterion necessary for terawatt-level deployment of thin-film PV technologies requires development of Earth-abundant solar absorbers.[4] One strategy to lower material cost is to replace the expensive elements with a combination of cheaper alternatives such that atomic and thus electronic structures are not significantly changed. This strategy, as applied to chalcopyrite CIGS, led to development of kesterite $Cu_2SnZn(S/Se)_4$ (CZTSSe),[5] both with tetrahedrally bonded structures related to zincblende ZnS. Although CZTSSe has recently been demonstrated in a 11% efficient cell,[6] its further development faces several challenges, including complex defect chemistry, strong tendency for disorder, and presence of compositional inhomogeneities.[4,7] These challenges have reenergized research on other Earth-abundant materials, such as SnS,[8–10] FeS_2,[11,12] Zn_3P_2,[13] and Cu_2O[14] binary materials and many ternary compounds.[15–17]

Here we adopt an alternative strategy to develop p-type solar absorbers. Instead of adhering to tetrahedral structural prototypes and increasing the chemical complexity, e.g., by mixing five different elements in CZTSSe (structure-specific approach), we consider the variety of different compounds that can be formed in different stoichiometries from a given set of three elements (element-specific approach), which in turn leads more rational selection of candidate materials and faster down-selection from these candidates. As an example, in this combined theoretical/experimental paper, we choose all known ternary Cu-Sn-S compounds and evaluate their (1) stability, (2) defect properties, and (3) electronic structure and optical properties. Our high-throughput evaluation identifies limitations of known members of Cu-Sn-S composition space and indicates that the Cu_2SnS_3 is the most viable solar absorber among the Cu-Sn-S compounds, despite its relatively small band gap of less than 1 eV. This conclusion is consistent with a remarkable cell efficiency of 6% that has recently been achieved with Cu_2SnS_3 based absorber[18] where a modest addition Ge led to a slight increase of the band gap energy E_g and improvement of other properties.

One advantage of this alternative approach is that it facilitates more rational design of the materials starting from selection of elements, without the limitations imposed by specific crystal structures. As an example, here for the evaluation we chose the Cu-Sn-S composition space because it is spanned by the Earth abundant elements and because we expect desirable properties such as p-type conductivity (due to high valence band energy from Cu(d) and S(p) states), high mobility of minority carriers (due to dispersive conduction band formed from Sn(s) states), and band gaps of $\sim$1 eV.[19–26] The Cu-Sn-S compounds reported in the crystallographic databases, such as Inorganic Crystal Structure Database (ICSD) and Powder Diffraction File (PDF), have Cu in a +1 and/or +2 (formal) oxidation state. We exclude from the evaluation Cu_4SnS_6, the only Cu-M-S compound with Cu being exclusively in a +2 oxidation state, as it has been reported to be metallic,[27] similar to electronically and structurally related CuS.[28] We also exclude sulfides with Cu in mixed valence states such as $Cu_{10}Sn_2S_{13}$,[20] Cu_3SnS_4,[19] or $Cu_5Sn_2S_7$[21] because multi-valency of Cu is likely to lead to either high hole density of $\sim 10^{22}\,cm^{-3}$ or hole trapping, both unfavorable for a solar absorber. For the detailed evaluation in this work, we therefore select four known Cu-Sn-S compounds in which Cu has a +1 oxidation state. Their compositions can be represented on the pseudobinary phase diagram Cu_2S–SnS_2: Cu_4SnS_4 (67% mol Cu_2S), Cu_2SnS_3 (50% mol Cu_2S), $Cu_4Sn_7S_{16}$ (22% mol Cu_2S), and $Cu_4Sn_{15}S_{32}$ (12% mol Cu_2S). We note that the fifth Cu-Sn-S compound $Cu_2Sn_3S_7$ that appears on pseudobinary phase diagram in Ref. 22 was redetermined to be $Cu_4Sn_7S_{16}$.[29]

Among the four compounds along the Cu_2S–SnS_2 tie-line, Cu_2SnS_3 (50% mol Cu_2S) has the most simple zincblende-related structure with cation sites that are

a)Electronic mail: andriy.zakutayev@nrel.gov
b)Electronic mail: stephan.lany@nrel.gov

four-fold coordinated by sulphur and vice versa. Depending on cation order controlled by temperature (T) Cu_2SnS_3 can have monoclinic *Cc* (low T, ordered[30]), cubic $F\bar{4}3m$ (high T, disordered[19]), or tetragonal $I\bar{4}2m$ (intermediate T, partially ordered) space group symmetry. The Cu_2SnS_3 compounds have equal numbers of cations and anions, similar to conventional semiconductors such as Si, GaAs, CdTe, $CuInSe_2$, Cu_2ZnSnS_4, etc. In contrast, the more Cu_2S-rich (SnS_2-poor) compound Cu_4SnS_4 (Pnma), has more cations than anions, and assumes a complex crystal structure with three distinct Cu sites that are separated from each other by less than 3 Å (the right panel of Fig. 3). The structures of the Cu_2S-poor (SnS_2-rich) compounds $Cu_4Sn_7S_{16}$ ($R\bar{3}m$) and $Cu_4Sn_{15}S_{32}$ ($F\bar{4}3m$) have more anions than cations and can be derived from the AB_2X_4 spinel structure with both tetrahedrally and octahedrally coordinated cation sites. In $Cu_4Sn_7S_{16}$, the tetrahedral A sites are 3/4 occupied by Cu atoms, 7/8 of the octahedral B sites are occupied by Sn, and 1/8 of them are occupied by Cu[29,31] and the rest of them are vacant; $Cu_4Sn_{15}S_{32}$ has half of tetrahedral sites occupied by Cu and 15/16 octahedral sites occupied by Sn.

Density functional theory with onsite Coulomb potential (DFT + *U*) calculations were performed with Perdew-Burke-Ernzerhof (PBE) exchange-correlation functional[32] within the projector augmented wave (PAW) formalism as implemented in the VASP code.[33] An effective on-site potential[34] $U = 5$ eV was applied to Cu *d* states. The fitted elemental reference energies (FERE)[35,36] were used for the calculation of the thermodynamic stability, which improves the accuracy of the calculated compound formation enthalpies to about 50 meV/atom.[36] Band gaps were calculated within *GW* approximation[37] following the approach of Ref. 38, where the DFT + *U* wavefunctions are maintained, but the eigenenergies are iterated to self-consistency. In order to compensate for the overestimated *d*-orbital energies in *GW*,[38] an on-site *d*-state potential of $V_d = -2.8$ eV was applied to the Cu-*d* states. This setting reproduces well the band gaps of the related chalcopyrites, e.g., $CuGaS_2$ and $CuInS_2$. (Note that uncertainties in the order of 0.2 eV in the predicted band gap energies remain even for main group compounds and somewhat larger uncertainties should be expected for electronically more complex transition metal compounds.[38]) The optical absorption spectra were calculated from the *GW* dielectric function in the independent particle approximation. Defect calculations for copper vacancies were performed using supercells of about 100 atoms. Since defect formation energies are critically dependent on proper positioning of band edges,[39] we used the valence band maximum and conduction band minimum values from *GW* calculations for the defect calculations. Electrostatic image charge and band filling[40] corrections were applied to account for finite size effects. The charge self-trapping energy was calculated using the methodology described in Ref. 41.

Thin films were synthetized using a high-throughput combinatorial approach, in which (a) an intentional and controlled spatial gradient of chemical composition is created across the substrate, (b) resulting sample libraries are characterized with spatial resolution, and (c) the data is semi-automatically analyzed.[42] In this study, the Cu-Sn-S thin films were deposited using angled co-sputtering from 50 mm diameter Cu_2S and SnS_2 targets on 50×50 mm stationary non-rotated glass substrates.[43] The cation compositional gradients were controlled by both[43] changing the relative Cu_2S/SnS_2 power ratio and the substrate temperature (50/50 W and 475 °C for Cu-poor, 50/25 W and 500 °C for Cu-rich). Each of the resulting combinatorial libraries was automatically mapped at 44 points (4×11 grid) to find the properties of the material as a function of chemical composition.[44] The samples were characterized using x-ray fluorescence (XRF) to determine the film thickness and Cu/Sn ratio, x-ray diffraction (XRD) to determine the phases present and their crystal structures, optical transmittance and reflectance, and a four point probe technique to determine sheet resistance. The resulting experimental data were analyzed using custom user functions written in the Igor-Pro software package. For this analysis, the measured thickness-dependent optical and electrical properties were combined with film thickness from XRF to obtain thickness independent absorption coefficient and conductivity values. These thickness independent properties were correlated with cation ratios and crystal structures. See supplementary material[45] for more details on computations and experiments.

Figure 1 shows the calculated chemical potential stability range for the Cu-Sn-S compounds of interest. Cu_2SnS_3 has the widest chemical potential stability range. On the Cu-rich side, Cu_2SnS_3 borders with Cu_2S through a narrow region of Cu_4SnS_4 at S-poor end or with CuS through Cu_3SnS_4 at S-rich end. On the Sn-rich side the neighboring compounds are SnS (S-poor end) or SnS_2 through $Cu_4Sn_7S_{16}$ (S-rich end). Our calculation finds $Cu_4Sn_7S_{16}$ and $Cu_4Sn_{15}S_{32}$ compounds to be marginally unstable with respect to Cu_2SnS_3 and SnS_2. One possible explanation that these compounds are reported in literature as stable is that they are stabilized at higher temperatures by entropic effects such as lattice vibrations or structural disorder, whereas our stability diagram (Fig. 1) is based on the enthalpy of formation, which is almost temperature independent. Such high temperature effects are indeed evident for $Cu_4Sn_7S_{16}$ which has a characteristic mushroom-shaped stability range at 500–680 °C in the experimental bulk temperature-composition phase diagram.[22] Note that the metallic, mixed-valence compound Cu_3SnS_4 has also a zinc-blende derived structure (modeled here in an 8 atom unit cell) like Cu_2SnS_3, and might be difficult to identify if it exists as an impurity phase.

The results of x-ray diffraction experiments shown in Fig. 2(a) are consistent with the theoretical thermodynamic stability calculations for the S-poor conditions (yellow dashed line in Fig. 1). With increasing Cu content, the observed phase assemblage changes from two-phase SnS/Cu_2SnS_3 to cubic Cu_2SnS_3, then through Cu_2SnS_3/Cu_4SnS_4 to Cu_4SnS_4, and finally through Cu_4SnS_4/Cu_2S to Cu_2S. Note that the phase pure cubic Cu_2SnS_3 is formed at more Sn-rich composition [$0.52 < x(Cu) < 0.62$] than expected [$x(Cu) = 0.67$], which may be caused by a systematic error of the XRF measurements (up to 5% for Sn-containing compounds). At the composition expected to produce phase pure Cu_4SnS_4 [$x(Cu) = 0.80$], no Cu_2SnS_3 or Cu_2S secondary phases were present according to XRD. We have not detected $Cu_4Sn_7S_{16}$ or $Cu_4Sn_{15}S_{16}$ in the deposited films, most likely because the

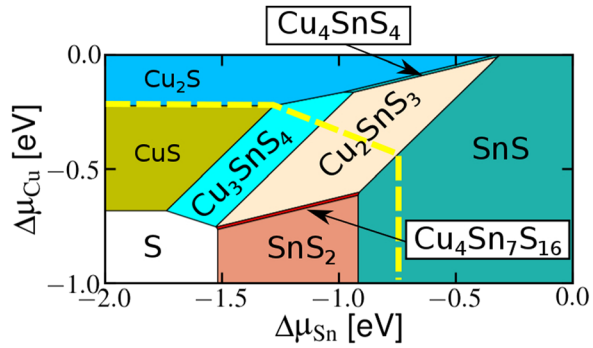

FIG. 1. Calcualted chemical potential phase space of Cu-Sn-S system. $\Delta\mu$ measures the atomic chemical potentials relative to the respective elemental phase. The wider bars indicate the location of the Cu_4SnS_4 and $Cu_4Sn_7S_{16}$ phases, which are marginally stable and marginally unstable, respectively. The dashed line indicates the upper bound $\Delta\mu_S \leq -0.46$ eV for the sulfur chemical potential in the present deposition method, i.e., only compounds to the right and above of the dashed line were observed in experiment.

sputter deposition was performed in S-poor environment (Ar gas only), whereas theoretical phase diagram (Fig. 1) shows that these materials should be stable in S-rich conditions. Nevertheless, we include $Cu_4Sn_7S_{16}$ in further analysis, as it has been reported stable below 500 °C in Ref. 22.

Cu-vacancies are well-known as a common low-energy shallow acceptor-like defect, which play often an important role for the photovoltaics properties.[46–48] If their formation energy is sufficiently low, they can create the p-type doping in the absorber needed to form the p-n junction. A too low formation energy, however, these acceptor-like defects can lead to degenerate hole densities (as in Cu_2S[49]), to Fermi level pinning,[48] or to high densities of compensating donor-like defects with potentially deleterious gap states.[50] The absolute formation energy can be expressed by the location of the Fermi pinning level E_F^{pin}, i.e., the Fermi level at which the vacancy formation energy becomes zero.[48] Since the defect formation energy depends on the chemical potentials (cf. Fig. 1), E_F^{pin} depends on the growth conditions (from Cu-rich to Cu-poor) and spans a certain range.

In the three selected Cu-Sn-S compounds, the Cu vacancies form shallow acceptor states with low ionization energies (40–70 meV) that are suitable for p-type doping, but the formation energy of these acceptor-like defects varies between these materials. As a result of this difference (Fig. 3), the range of E_F^{pin} in $Cu_4Sn_7S_{16}$ extends fairly deep into the band gap region, indicating a high risk for the above-mentioned negative consequences for the photovoltaic properties. Although less pronounced, this behavior is also observed for the Cu_4SnS_4 phase. In case of Cu_2SnS_3, E_F^{pin} lies above the conduction band minimum, around 1.0–1.7 eV, thereby avoiding such pinning effects, even when alloyed with Ge[18] or Si,[51] which are expected to increase the band gap by raising the conduction band edge. The respective absolute vacancy formation energies in Cu_2SnS_3 would support p-type doping in the desirable range between 10^{15} and 10^{18} cm^{-3}; however, the actual doping levels will of course also depend on the presence of other types of defects (e.g., anti-sites, interstitials).

The experimental results for Cu-Sn-S materials (Fig. 2(b)) show large changes in electrical conductivity of nearly

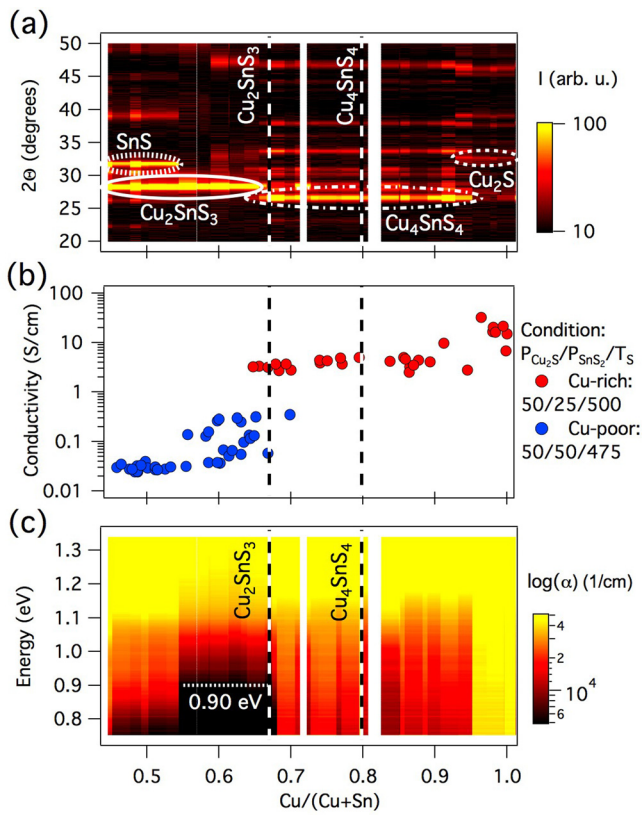

FIG. 2. Experimentally determined composition dependence of (a) structural (XRD), (b) electrical, and (c) optical properties of the Cu-Sn-S system. Vertical dashed lines indicate Cu_2SnS_3 and Cu_4SnS_4 nominal compositions.

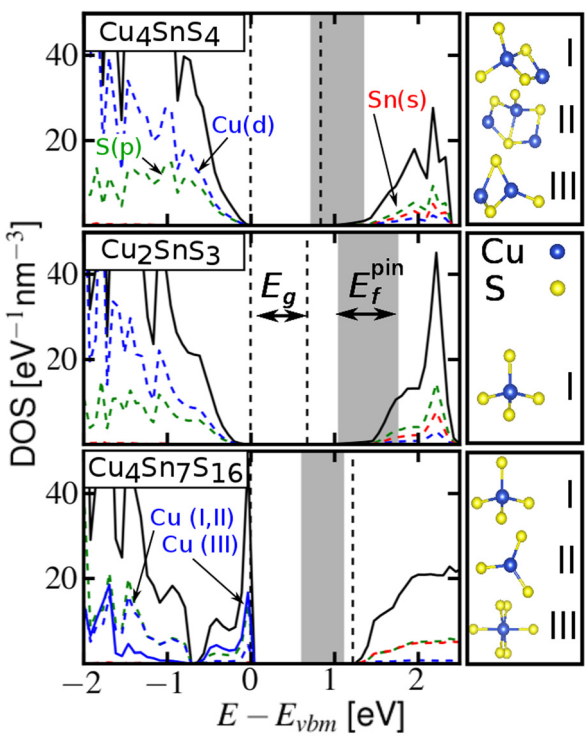

FIG. 3. Left panels: Volume-normalized calculated density of states and its projections onto atomic orbitals. Black dashed lines indicate valence and conduction band edges; shaded areas denote the range between the maximum (Cu-rich) and the minimum (Cu-poor) energies where Fermi level will be pinned due to spontaneous formation of Cu vacancies. Right panels: Local coordination of Cu atoms within 3 Å.

three orders of magnitude across the composition range of $Cu/(Cu+Sn)=0.5-1.0$. In the cubic Cu_2SnS_3 phase, the electrical conductivity ranges between 0.03 and 0.5 S/cm. Increasing Cu content causes an increase in electrical conductivity: the Cu_4SnS_4 phase shows intermediate values of conductivity (~3 S/cm), and the Cu_2S phase has the highest electrical conductivity (~ 20 S/cm). For the most part, we attribute large differences in conductivity of Cu-Sn-S materials to variations in hole density rather than hole mobility, because 2-3 orders of magnitude changes in mobility are unlikely for chemically related materials deposited under similar conditions. This trend and its explanation are consistent with the theoretically calculated differences in defect formation energies. We also note that the high conductivity of Cu_4SnS_4 suggests that this material as a photovoltaic absorber may face problems similar to those in Cu_2S.[49]

Cu_4SnS_4, Cu_2SnS_3, and $Cu_4Sn_7S_{16}$ have quite similar electronic structures. The conduction band is formed from antibonding Sn 5*s* and S 2*p* states (see Fig. 3), and the valence band is formed from antibonding Cu 3*d* and S 3*p* orbitals, similar as in Cu_2S, $CuInS_2$, or Cu_2ZnSnS_4 materials. The overall valence band density of states decreases with decreasing Cu content from Cu_4SnS_4 through Cu_2SnS_3 to $Cu_4Sn_7S_{16}$. A notable difference between $Cu_4Sn_7S_{16}$ and the other two compounds is that the top of the $Cu_4Sn_7S_{16}$ valence band is formed by a relatively narrow band with high density of states, which originates from the octahedrally coordinated Cu sites (see Fig. 3). This feature causes a high effective mass and suggests that $Cu_4Sn_7S_{16}$ may be prone to charge self-trapping (small polaron formation). Hole trapping is an undesirable feature of solar absorber as it may lead to increased recombination rates and short carrier lifetimes. We calculated hole self-trapping energy on octahedral Cu sites and found that the self-trapped state is almost degenerate in energy with the free hole state. These results suggest a possibility of poor hole transport properties in $Cu_4Sn_7S_{16}$.

In the *GW* calculations, Cu_2SnS_3 is found to be direct band gap semiconductors with band gap of 0.63 eV (Fig. 4). The corresponding experimental optical absorption threshold of 10^3–10^4 cm^{-1} ranges between 0.8 eV and 0.9 eV (Fig. 2(c)). Both theoretical and experimental values are somewhat lower than the previously reported experimental optical band gaps of 0.93–1.35 eV (Refs. 19–25) for Cu_2SnS_3. Cu_4SnS_4, for which we calculated direct gap at 0.82 eV, does not show a clear absorption threshold in experiment, most likely due to large sub-gap absorption and the high defect density that also causes high electrical conductivity (Fig. 2(b)). The theoretical and experimental absorption coefficients (Figs. 4 and 2(c), respectively) for Cu_2SnS_3 and Cu_4SnS_4 are high, reaching 10^5 cm^{-3} at 1.0 eV above the band gap. In contrast to Cu_2SnS_3 and Cu_4SnS_4, $Cu_4Sn_7S_{16}$ is an indirect band gap material with the calculated direct gap of 1.27 eV being slightly above the indirect gap of 1.23 eV. Its absorption coefficient near the absorption onset is smaller than for Cu_2SnS_3 or Cu_4SnS_4, perhaps due to the overall lower density of states in the valence band.

Overall, the evaluation indicates Cu_2SnS_3 as the most viable solar absorber among Cu-Sn-S materials with Cu in +1 oxidation state. While decrease in Cu/Sn ratio in CZTS and Cu_2SnS_3 has been correlated with improved solar absorber properties,[4,52] there is no clear trend with the Cu/Sn ratio among the compounds considered here. Both the Cu-rich Cu_4SnS_4 and the Cu-poor $Cu_4Sn_7S_{16}$ compounds have inferior properties compared to Cu_2SnS_3. Cu_4SnS_4 has too high experimental conductivities, and $Cu_4Sn_7S_{16}$ has low calculated absorption coefficient, poor hole transport, and Fermi level pinning due to Cu vacancy defects. In contrast, Cu_2SnS_3 has a wide thermodynamic stability window, a high absorption coefficient, and is resilient to the Fermi level pinning. Although Cu_2SnS_3 has a relatively small band gap, the respective solar cell efficiency in the Shockley-Queisser limit[53] lies still above 20%. While the band gap could be increased by alloying with Ge[18] or with Si[51] on the Sn site, we note that an increase of E_g in polycrystalline thin-film absorbers usually does not fully translate into a corresponding increase in the open-circuit voltage.[7,54] Thus, the practical efficiency maximum in inorganic thin-film photovoltaics can be expected to lie at relatively low band gap energies, as in the case of CIGS (rather than CGS) and CZTSe (rather than CZTS).

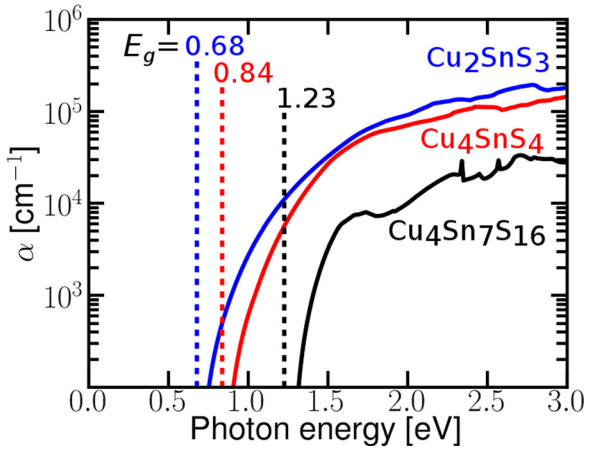

FIG. 4. Calculated optical absorption spectra for Cu_4SnS_4, Cu_2SnS_3, and $Cu_4Sn_7S_{17}$. Vertical dashed lines denote quasi-particle band gaps.

The example of Cu-Sn-S materials family presented in this work demonstrates an alternative element-specific (rather than structure-specific) way to search for Earth-abundant solar cell absorbers. The results of our comparative study of ternary Cu-Sn-S materials family clearly suggests Cu_2SnS_3 as the best candidate material for solar absorber applications and points out to potential problems with other members of this family such as too high electrical conductivity in Cu_4SnS_4 or poor hole mobility and Fermi level pinning in $Cu_4Sn_7S_{16}$. Thus, the present work has generated a clear understanding of the most critical issues in the individual Cu-Sn-S compounds, which forms the basis for further optimization of the PV materials in this composition space. Overall, the alternative element-specific approach exemplified in this work by Cu-Sn-S materials holds a promise to accelerate the development of photovoltaic technologies in the future.

This work was funded by the U.S. Department of Energy, office of Energy Efficiency and Renewable Energy, as a part of the "Rapid Development of Earth-abundant thin film solar cells" agreement. E.S.T. acknowledges support of

the NSF MRSEC program through the REMRSEC Center. L.L.B. acknowledges support of the Department of Defense (DoD) through National Defense Science and Engineering Graduate Fellowship (NDSEG) Program.

[1]P. Jackson, D. Hariskos, E. Lotter, S. Paetel, R. Wuerz, R. Menner, W. Wischmann, and M. Powalla, Prog. Photovoltaics **19**, 894 (2011).
[2]*Critical Materials Strategy*, U.S. Dept. of Energy, Washington DC (2010), available at http://energy.gov/sites/prod/files/DOE_CMS2011_FINAL_Full.pdf.
[3]*Critical Raw Materials for the EU*, European Commission (2010), available at http://ec.europa.eu/enterprise/policies/raw-materials/files/docs/report-b_en.pdf.
[4]S. Delbos, EPJ Photovoltaics **3**, 35004 (2012).
[5]K. Ito and T. Nakazawa, Jpn. J. Appl. Phys., Part 2 **27**, 2094 (1988).
[6]T. K. Todorov, J. Tang, S. Bag, O. Gunawan, T. Gokmen, Y. Zhu, and D. B. Mitzi, Adv. Energy Mater. **3**, 34 (2013).
[7]S. Siebentritt, Thin Solid Films **535**, 1 (2013).
[8]J. Vidal, S. Lany, M. d'Avezac, A. Zunger, A. Zakutayev, J. Francis, and J. Tate, Appl. Phys. Lett. **100**, 032104 (2012).
[9]A. Schneikart, H.-J. Schimper, A. Klein, and W. Jaegermann, J. Phys. D. Appl. Phys. **46**, 305109 (2013).
[10]P. Sinsermsuksakul, K. Hartman, S. Bok Kim, J. Heo, L. Sun, H. Hejin Park, R. Chakraborty, T. Buonassisi, and R. G. Gordon, Appl. Phys. Lett. **102**, 053901 (2013).
[11]R. Sun, M. K. Y. Chan, S. Kang, and G. Ceder, Phys. Rev. B **84**, 035212 (2011).
[12]M. Cabán-Acevedo, M. S. Faber, Y. Tan, R. J. Hamers, and S. Jin, Nano Lett. **12**, 1977 (2012).
[13]J. P. Bosco, D. O. Scanlon, G. W. Watson, N. S. Lewis, and H. A. Atwater, J. Appl. Phys. **113**, 203705 (2013).
[14]Y. Nishi, T. Miyata, and T. Minami, Thin Solid Films **528**, 72 (2013).
[15]M. Kumar and C. Persson, Appl. Phys. Lett. **102**, 062109 (2013).
[16]M. Yang, A. Zakutayev, J. Vidal, X. Zhang, D. S. Ginley, and F. J. DiSalvo, Energy Environ. Sci. **6**, 2994 (2013).
[17]L. Yu, S. Lany, R. Kykyneshi, V. Jieratum, R. Ravichandran, B. Pelatt, E. Altschul, H. a. S. Platt, J. F. Wager, D. A. Keszler, and A. Zunger, Adv. Energy Mater. **1**, 748 (2011).
[18]M. Umehara, Y. Takeda, T. Motohiro, T. Sakai, H. Awano, and R. Maekawa, Appl. Phys. Express **6**, 045501 (2013).
[19]P. A. Fernandes, P. M. P. Salomé, and A. F. da Cunha, Phys. Status Solidi C **7**, 901 (2010).
[20]D. Avellaneda, M. T. S. Nair, and P. K. Nair, J. Electrochem. Soc. **157**, D346 (2010).
[21]Z. Su, K. Sun, Z. Han, F. Liu, Y. Lai, J. Li, and Y. Liu, J. Mater. Chem. **22**, 16346 (2012).
[22]S. Fiechter, M. Martinez, G. Schmidt, W. Henrion, and Y. Tomm, J. Phys. Chem. Solids **64**, 1859 (2003).
[23]M. Bouaziz, J. Ouerfelli, S. K. Srivastava, J. C. Bernede, and M. Amlouk, Vacuum **85**, 783 (2011).
[24]M. Adelifard, M. M. B. Mohagheghi, and H. Eshghi, Phys. Scr. **85**, 35603 (2012).
[25]D. M. Berg, R. Djemour, L. Gutay, S. Siebentritt, P. J. Dale, X. Fontane, V. Izquierdo-Roca, and A. Perez-Rodriguez, Appl. Phys. Lett. **100**, 192103 (2012).
[26]M. T. S. Nair, C. Lopez-Mata, O. GomezDaza, and P. K. Nair, Semicond. Sci. Technol. **18**, 755 (2003).
[27]X.-a. Chen, H. Wada, and A. Sato, Mater. Res. Bull. **34**, 239 (1999).
[28]H. Nozaki, K. Shibata, and N. Ohhashi, J. Solid State Chem. **91**, 306 (1991).
[29]X. Chen, H. Wada, A. Sato, and M. Mieno, J. Solid State Chem. **139**, 144 (1998).
[30]Y.-T. Zhai, S. Chen, J.-H. Yang, H.-J. Xiang, X.-G. Gong, A. Walsh, J. Kang, and S.-H. Wei, Phys. Rev. B **84**, 75213 (2011).
[31]J. P. F. Jemetio, P. Zhou, and H. Kleinke, J. Alloys Compd. **417**, 55 (2006).
[32]J. P. Perdew, K. Burke, and M. Ernzerhof, Phys. Rev. Lett. **78**, 1396 (1997).
[33]G. Kresse and D. Joubert, Phys. Rev. B **59**, 1758–1775 (1999).
[34]S. L. Dudarev, G. A. Botton, S. Y. Savrasov, C. J. Humphreys, and A. P. Sutton, Phys. Rev. B **57**, 1505 (1998).
[35]S. Lany, Phys. Rev. B **78**, 245207 (2008).
[36]V. Stevanović, S. Lany, X. Zhang, and A. Zunger, Phys. Rev. B **85**, 115104 (2012).
[37]M. Shishkin and G. Kresse, Phys. Rev. B **74**, 035101 (2006).
[38]S. Lany, Phys. Rev. B **87**, 085112 (2013).
[39]H. Peng, D. O. Scanlon, V. Stevanovic, J. Vidal, G. W. Watson, and S. Lany, Phys. Rev. B **88**, 115201 (2013).
[40]S. Lany and A. Zunger, Modell. Simul. Mater. Sci. Eng. **17**, 84002 (2009).
[41]S. Lany and A. Zunger, Phys. Rev. B **80**, 85202 (2009).
[42]A. Zakutayev, F. J. Luciano, V. P. Bollinger, A. K. Sigdel, P. F. Ndione, J. D. Perkins, J. J. Berry, P. A. Parilla, and D. S. Ginley, Rev. Sci. Instrum. **84**, 053905 (2013).
[43]A. Zakutayev, J. D. Perkins, P. A. Parilla, N. E. Widjonarko, A. K. Sigdel, J. J. Berry, and D. S. Ginley, MRS Commun. **1**, 23 (2011).
[44]A. Zakutayev, T. R. Paudel, P. F. Ndione, J. D. Perkins, S. Lany, A. Zunger, and D. S. Ginley, Phys. Rev. B **85**, 085204 (2012).
[45]See supplementary material at http://dx.doi.org/10.1063/1.4851896 for more details on computations and experiments.
[46]A. Klein and W. Jaegermann, Appl. Phys. Lett. **74**, 2283 (1999).
[47]R. Caballero, C. a Kaufmann, M. Cwil, C. Kelch, D. Schweigert, T. Unold, M. Rusu, H. W. Schock, and S. Siebentritt, J. Phys. Condens. Matter **19**, 356222 (2007).
[48]C. Persson, Y. Zhao, S. Lany, and A. Zunger, Phys. Rev. B **72**, 35211 (2005).
[49]L. D. Partain, P. S. McLeod, J. A. Duisman, T. M. Peterson, D. E. Sawyer, and C. S. Dean, J. Appl. Phys. **54**, 6708 (1983).
[50]S. Lany and A. Zunger, Phys. Rev. Lett. **100**, 016401 (2008).
[51]Y. Chang, L. Fang-Yang, L. Yan-Qing, L. Jie, and L. Ye-Xiang, Chin. Phys. Lett. **28**, 108801 (2011).
[52]J. Koike, K. Chino, N. Aihara, H. Araki, R. Nakamura, K. Jimbo, and H. Katagiri, Jpn. J. Appl. Phys. **51**, 10NC34 (2012).
[53]W. Shockley and H. J. Queisser, J. Appl. Phys. **32**, 510 (1961).
[54]R. Kniese, M. Lammer, U. Rau, and M. Powalla, Thin Solid Films **451–452**, 430 (2004).